



ISSN: 0067-2904

Enhancing of Corrosion Protection of Steel Rebar in Concrete Using TiO₂ Nanoparticles as Additive

Noor Ali Khudhair, Abdulkareem M.A. Al-Sammarraie*

Department of Chemistry, College of Science, University of Baghdad, Baghdad, Iraq

Abstract

Nanomaterials became targeted materials for many important applications due to its huge surface area and quantum confinement effects. In this work TiO₂ nanoparticles (30nm) were used as additive to enhance the corrosion protection of steel rebar in artificial concrete solution (Ca(OH)₂ (2g), KOH (22.44mg), NaOH (8mg) in 1L of distilled water) against saline environment (3.5%NaCl) at four temperatures; 20, 30, 40, and 50°C. Three different concentrations of TiO₂ NPs were used namely; 1, 3, and 5% by weight. The corrosion parameters and pitting probability were followed using Tafel and cyclic polarization plots respectively. Protection enhancement was recorded at all TiO₂ percent used and efficiencies of 75-86% were achieved. Using TiO₂ NPs reduces but not diminished the pitting hysteresis loop area. The results supported by surface morphology examination using atomic force microscope (AFM).

Keywords: Corrosion inhibition, Nanomaterials, Steel rebar, Saline, TiO₂

تعزيز الحماية من التآكل لحديد التسليح في الخرسانة بإضافة جسيمات ثنائي أكسيد التيتانيوم النانوية

نور علي خضير، عبدالكريم محمد علي السامرائي*
قسم الكيمياء، كلية العلوم، جامعة بغداد، بغداد، العراق

الخلاصة

أصبحت المواد النانوية مواد مطلوبة للعديد من التطبيقات المهمة بسبب مساحتها السطحية الفائقة وتأثيراتها على الاحتجاز التكمي. تم في هذا العمل استخدام جسيمات TiO₂ النانوية (30 نانومتر) كمضافه لتعزيز حماية تآكل حديد التسليح من التآكل في محلول الخرسانة الاصطناعي (Ca(OH)₂ (2g)، KOH (22.44mg)، NaOH (8mg) في 1 لتر من الماء المقطر) ضد البيئة المالحة (3.5% كلوريد الصوديوم) في أربع درجات حرارة؛ 20 و 30 و 40 و 50 درجة مئوية. وتم استخدام ثلاثة تراكيز مختلفة من جسيمات ثنائي أكسيد التيتانيوم النانوية (1 و 3 و 5) % وزنيا. وجرى متابعة معاملات التآكل واحتمال التآكل التقري باستخدام منحنيات Tafel والاستقطاب الرجوعي على التوالي. وقد تم الحصول على نسب جيدة للحماية من التآكل عند كل نسب TiO₂ المستخدمة مع تحقيق كفاءة تراوحت بين 75-86%. لوحظ حصول تقلص لمساحة منطقة التآكل عند استخدام جسيمات ثنائي أكسيد التيتانيوم النانوية دون أن يتم التخلص من كل منطقة التآكل ضمن الحلقة الرجوعية. وقد تم تدعيم النتائج بواسطة فحص تضاريس السطح بواسطة مجهر القوة الذرية.

*Email: karim.alsamuraee@gmail.com

Introduction

Corrosion of steel rebar in concrete is one of the major research areas that has been attracting the attention over long times since it is recognized as a problem causing degradation, failure, and serious accidents and hazards in much structural concrete building [1,2]. This deterioration of the concrete objects due to their reaction with corrosive environments surroundings, such as chlorine, carbon dioxide, etc. [3, 4]. Many approaches were used to overcome or decreases the risk of concrete corrosion [5-7], such as using additives to the concrete mix [8, 9], coating the steel rebar, and others [10, 11].

In the past 10 years, nanotechnology has become one of the most important methods used in many applications, the most important of which is the protection from corrosion. Many materials have been used for this purpose, such as ceramic materials and others [12-14].

The present work aimed to study the influence of using TiO₂ NPs as additive to the artificial concrete solution on the corrosion properties of the steel rebar in saline environment (3.5% NaCl).

Materials and methods:

The chemical composition of the steel rebar which is used in this study is given by the manufacturer and listed in Table-1

Table 1- Chemical composition of steel rebar

Element	C	S	Si	N	Cu	Mn	Ni	Cr
%	0.26	0.031	0.28	0.010	0.28	0.73	0.13	0.12

First the steel rebar was pickled with concentrated HCl (37%, Fluka/ Switzerland), followed by rinsing with tap water and then with ethanol and dried well, the rebar was then covered with adhesive tape except for a known area which is (16.55cm²) and was immersed in three electrode cell and serve as working electrode, the Pt-electrode serve as counter electrode, and Ag/AgCl as references electrode. TiO₂ NPs (50nm, MTI, USA) were used to enhance the corrosion protection properties by two ways of application; first as an additive in different concentration (1, 3, and 5%) and second by coating the steel rebar with TiO₂ NPs. Then the steel rebar polarized in the concrete simulation solution (Ca(OH)₂ (2g), KOH (22.44mg), NaOH (8mg) in 1L of distill water containing 3.5% NaCl) at different temperatures (20, 30, 40 & 50 °C). Then, Tafel plots were recorded for corrosion rate measurement by scanning the potentials ±200mv around the open circuit potential (OCP) with a rate of 2mv/sec. The same procedure repeated at four temperatures; 20, 30, 40, and 50°C.

The cyclic polarization conducted at 20°C starting from few millivolts lower than OCP going up to about 1000mv.

The change in the morphology of the steel rebar surface before and after polarization was followed by Atomic Force Microscope (SPM AA3000, Angstrom Advanced Inc., USA).

Results and discussion:

Figure-1 shows the recorded Tafel plots for the steel rebar in a simulated concrete solution containing TiO₂ NPs (1%, 3%, and 5%) and 3.5% NaCl, at temperatures of 20, 30, 40, and 50°C.

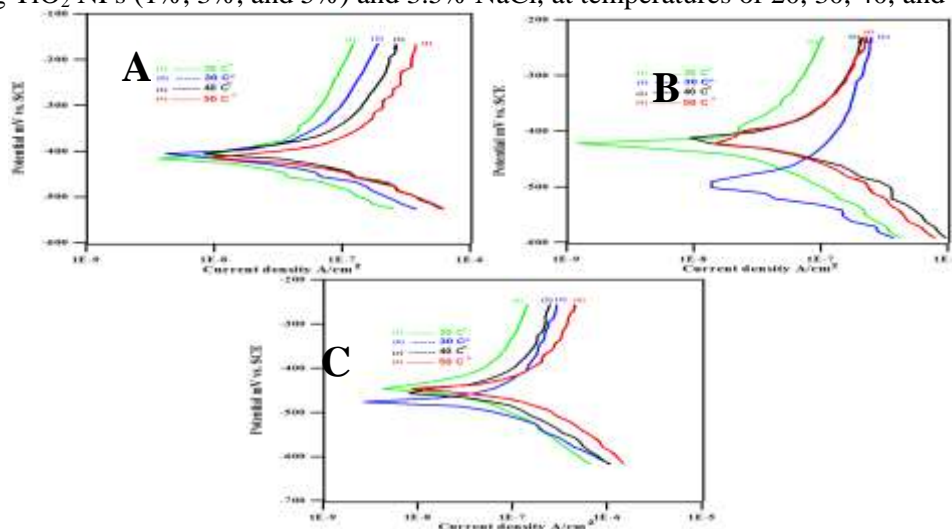


Figure 1-Tafel plots of steel rebar polarized in simulated concrete solution containing TiO₂ NPs (A-1.0 %, B-3.0 %, and C-5.0 %) at 3.5% NaCl and different temperatures.

Table-2 summarizes all calculated corrosion parameters and Table-3 presents the calculated thermodynamic functions for steel rebar in artificial concrete solution with different concentrations of TiO₂ and 3.5% NaCl.

The polarization resistance was calculated using Equation 1:

$$R_p = \frac{\beta_a \beta_c}{2.303 (i_{corr})(\beta_a + \beta_c)} \quad (1)$$

Where β_a and β_c are Tafel slopes and i_{corr} is the corrosion current. In comparisons with the corrosion rates measured without using TiO₂ NPs the protection efficiencies were measured using the following equation [15]:

$$PE\% = [(CR_0 - CR_x) / CR_0] * 100 \quad (2)$$

Where CR₀ and CR_x are the corrosion rate without and with using NPs respectively.

Table 2- Corrosion rate parameters of steel rebar polarized in simulated concrete solution containing TiO₂ Nps (30nm) and 3.5% NaCl at 20, 30, 40, 50°C.

TiO ₂ %	T (K)	E _{corr} (mV)	i _{corr} (A*10 ⁻⁶ /cm ²)	B _c (mV/Dec)	β _a (mV/Dec)	R _p Ω.cm ²	CR(WL) g.m ⁻² d ⁻¹	CR(PL) mmpy	PE%
0	293	-458.7	95.86	-125.1	145.5	304.69	24	1.110	---
	303	-478.1	100.76	-91.6	102.1	208.07	25.2	1.170	----
	313	-467.8	215.79	97.6-	176.3	126.41	53.9	2.500	----
	323	-457.1	257.57	-123.6	142.3	111.51	64.4	2.990	----
1	293	-413.5	22.74	-108.1	217.7	1379.26	5.68	0.264	76.21
	303	-408.2	25.70	-95.8	152.6	994.35	6.43	0.298	74.52
	313	-401.0	32.37	-86.8	120.2	676.10	8.09	0.376	84.96
	323	-414.5	39.16	-79.2	111.4	513.27	9.79	0.454	84.81
3	293	-422.7	17.79	-101.5	170.9	1554.28	4.45	0.207	81.35
	303	-493.2	23.93	-73.6	97.3	760.34	5.98	0.278	76.23
	313	-415.5	30.75	-73.4	111.5	625.02	7.69	0.357	85.72
	323	-415.5	38.15	-101.3	147.0	682.59	9.54	0.443	85.18
5	293	-441.3	14.10	-67.9	80.5	1134.27	3.52	0.164	85.22
	303	-478.3	22.45	-51.9	77.2	600.27	5.61	0.261	77.69
	313	-455.5	28.56	-68.5	98.6	614.52	7.14	0.332	86.72
	323	-446.6	36.44	-59.1	69.5	380.59	9.11	0.423	85.85

The data in Table-2 reflected that all percent of TiO₂ NPs which have been added to the concrete solution, succeeded to enhance the protection efficiency more than 75% and reach a maximum of 86% with using 5% TiO₂.

The values of R_p steel rebar in concrete solution without using nanoparticles as additive decreased with increasing temperature which attributed to the formation of corrosion product (Iron oxides), while R_p for steel rebar in concrete solution containing TiO₂ NPs have high values than the values before adding TiO₂ NPs and decrease with increasing temperature at all temperature which mean no corrosion products was formed on steel bar surface[16, 17]. The kinetics properties (E_a, ΔG*, ΔH*, and ΔS*) were calculated using the following relationships [18]:

$$\text{Log CR} = \text{log A} - \frac{E^*}{2.303RT} \quad (3)$$

$$\text{Log} \frac{CR}{T} = \text{log} \left(\frac{R}{N_h} \right) + \frac{\Delta S^*}{2.303R} - \frac{\Delta H^*}{2.303RT} \quad (4)$$

Where R is the universal gas constant (8.314 J mol⁻¹ K⁻¹), T is the temperature in K, h is the Plank's constant (6.626176 x 10⁻³⁴ Js), N is the Avogadro's number (6.022 x 10²³ mol⁻¹), ΔS*_i is the entropy of activation and ΔH* is the enthalpy of activation. Then ΔG* was calculated using Equation (5).

$$\Delta G^* = \Delta H^* - T\Delta S^* \tag{5}$$

All kinetics and thermodynamic functions are tabulated in Table-3.

Table -3 Kinetics and thermodynamic parameters of steel rebar corrosion in /concrete electrolyte solution containing 3.5% NaCl and TiO₂ NPs.

TiO ₂ %	T(K)	Ea (kJ/mole)	ΔH* (kJ/mol)	ΔS* (kJ/mol.K)	ΔG* (kJ/mol)
0	293	16.090	18.569	-0.144	60.761
	303				62.201
	313				63.641
	323				65.081
1	293	14.258	9.066	-0.188	64.15
	303				66.03
	313				67.91
	323				69.79
3	293	20.012	12.878	-0.176	64.446
	303				66.206
	313				67.966
	323				69.726
5	293	24.907	16.790	-0.164	64.842
	303				66.482
	313				68.122
	323				69.762

The values of activation energy Ea* increased with increasing TiO₂ content due to increasing the surface area of the nanoparticles that dispersed in the concrete solution [19].

The activation enthalpy of the transition process (ΔH*) took positive value which indicating endothermic reaction and also increased with increasing TiO₂. The entropy (ΔS*) reflect the change in the order and orientation of the solvent molecules around the hydrated metal ions in the corrosion medium then metal atoms were corroded and subsequently hydrated in the solution [20]. Since the activation Gibbs free energy (ΔG*) seems to be nearly constant and have positive value at all temperature which describes the process also as non-spontaneous one for transition reaction [21]. The surface morphology changing was tested by Atomic force microscope, as shown in Figure-2

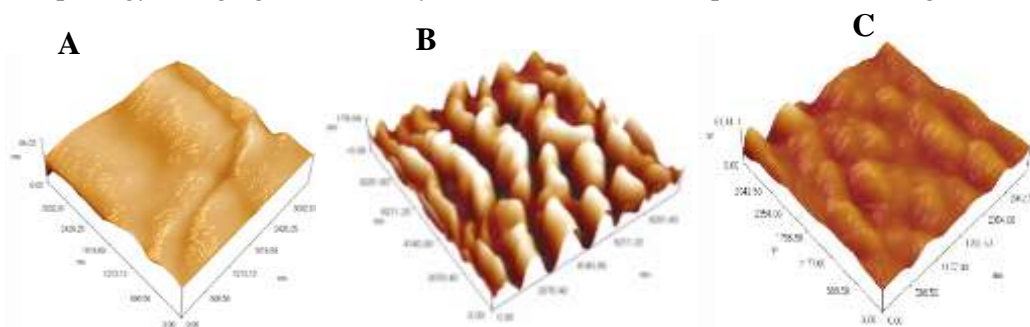


Figure 2- AFM 3D views of steel rebar after polarization in artificial concrete solution containing; A- without any additives, B- containing 3.5% NaCl , and C- containing 3.5% NaCl and 5% TiO₂ NPs,

These images clearly supported the investigations deduced from the electrochemical polarization procedure, since the surface morphology in 3.5% NaCl without using TiO₂ is very rough containing deep valley (Figure-2B), while the roughness after using TiO₂ as additive seems to be unaffected (Figure-2C) in comparisons with the roughness of the steel bar before polarization process (Figure-2A).

The probability of pitting corrosion occurrences was investigated by cyclic polarization procedure [22] as mentioned in the experimental part, Figure-3 show the cyclic Voltgrams and the histories loops which have formed during the polarization in each solution.

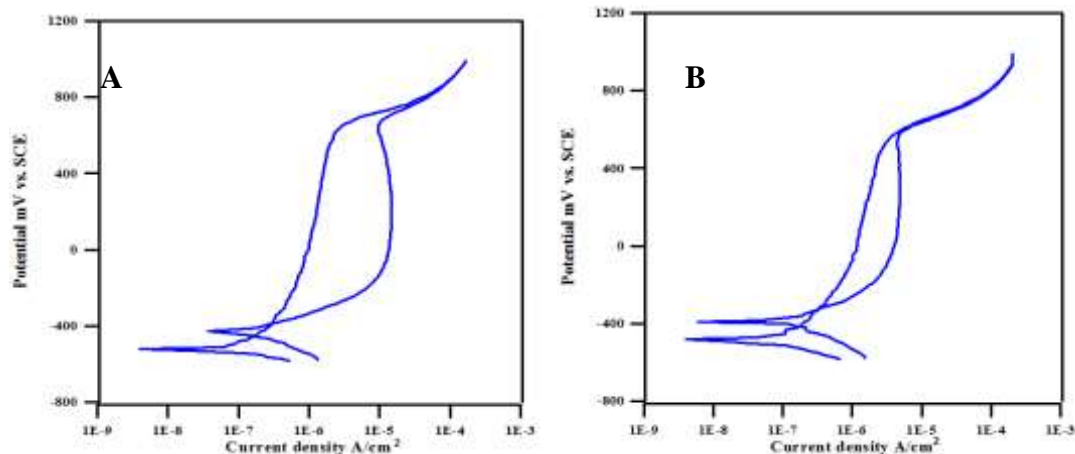


Figure 3- Cyclic polarization voltgram of steel rebar polarized in artificial concrete solution containing 3.5% NaCl; a-without TiO₂ NPs, b- with TiO₂ NPs as additive at 20°C.

Unfortunately, this polarization Voltgrams show that the TiO₂ NPs reduces the pitting area but not fully diminished the pitting problem of the chloride ions.

Conclusions:

The results indicated the following conclusions on adding TiO₂ NPs to the concrete;

- i- enhanced the corrosion protection of the steel bar against seawater condition,
- ii- TiO₂ NPs reduces but not diminished the pitting hysteresis loop area.

References

1. Jun L., Guangfeng O., Qiwen Q., Xiaochi C., Jing H. and Feng X. **2017**. Corrosion Protection of Carbon Steel By Voltaren Drug in Acid Media and Theoretical Studies. *C&BM*, **146**(15):493-501.
2. Sanjeev, K.V., Sudhir, S.B. and Saleem A. **2014**. Monitoring Corrosion of Steel Bars in Reinforced Concrete Structures. *SWJ*, 9 pages. doi.org/10.1155/2014/957904
3. Michael T. **1996**. Chloride thresholds in marine concrete. *C&CR*, **26**(4): 513-519. [doi.org/10.1016/0008-8846\(96\)00035-X](https://doi.org/10.1016/0008-8846(96)00035-X)
4. Li M., and Li, V.C. **2011**. Cracking and healing of engineered cementitious composites under chloride environment. *ACIMJ*, **108**(3): 333-340.
5. Paul S., and Van Z.G. **2017**. Corrosion deterioration of steel in cracked SHCC. *I JCS&M*, **11**(3): 557-572. doi.org/10.1007/s40069-017-0205-8
6. Zhao, X., Chen, C., Xu, W., Zhu Q. and Ge C. **2016**. Evaluation of long-term corrosion durability and self-healing ability of scratched coating systems on carbon steel in a marine environment. *CJO&L*, 1-14. doi.org/10.1007/s00343-017-6132-3
7. Mihashi, H.S., and Ahmed, K.A. **2011**. Corrosion of reinforcing steel in fibre reinforced cementitious composites. *JACT*, **9**(2): 159-167. doi.org/10.3151/jact.9.159
8. Magdalena O., Daniel W. **2016**. Organic substances as corrosion inhibitors for steel in concrete – an overview, *J. Build. Chem.*, **1**: 42-53.
9. Goyal, A. Sadeghi, P.H. Ganjian E. and Claisse P.A. **2018**. Review of corrosion and protection of steel in concrete. *AJFS&E*, **43**(10): 5035-5055.
10. Bentur, A., Diamond, S. and Berke, N.S. **1997**. *Steel Corrosion in Concrete*, London: E & FN Spon. <https://hrcak.srce.hr/50007>

11. Raheema A.C. and Umesh K.S. **2019**. Influence of temperature and relative humidity variations on non-uniform corrosion of reinforced concrete, *Structures*. **19**(6): 296-308. doi.org/10.1016/j.istruc.2019.01.016
12. Laila, R., James, B., Rouhollah, A., Jon, M. and Taijiro S. **2010**. Cement and concrete nanoscience and nanotechnology. *Materials*, **3**: 918-942. doi.org/10.3390/ma3020918
13. LinK, L., Chang, W.C., Lin, D.F., Luo, H.L. and Tsai, M.C. **2008**. Effects of nano-SiO₂ and different ash particle sizes on sludge ash–cement mortar. *J. Environ. Manag.* **88**: 708–714. doi.org/10.1016/j.jenvman.2007.03.036
14. Sato, T. and Beaudoin J.J. **2007**. The Effect of nano-sized CaCO₃ addition on the hydration of cement paste containing high volumes of fly ash. In *Proceedings of the 12th International Congress on the Chemistry of Cement, Montreal, Canada*, 8–13 July: 1–12.
15. Rawaa, A.M. and Dunya, E. **2019**. Using natural materials as corrosion inhibitors for carbon-steel on phosphoric acid medium, *IJS, Special Issue*, 40-45. <http://scbaghdad.edu.iq/eijs/index.php/eijs/article/view/645>
16. Doua'a, A.A. **2015**. *Corrosion Protection of Steel Using Nano Ceramic Particles Coating*, Thesis, university of technology, Baghdad, Iraq.
17. Shen, G.X., Chen, Y.C., Lin, L., Lin, C.J. and Scantlebury, D. **2005**. Study on a hydrophobic nano TiO₂ coating and its properties for corrosion protection of metals. *ECA*, **50**(25-26): 5083–9. doi.org/10.1016/j.electacta.2005.04.048
18. Kaesche, H. **2003**. *Chemical Thermodynamics of Corrosion*. In: *Corrosion of Metals*. Engineering Materials and Processes. Springer, Berlin, Heidelberg.
19. Xiong, G., Deng, M., Xu, L. and Tang, M. **2006**. Properties of cement-based composites by doping nanoTiO₂. *J. Chin. Ceram. Soc.* **34**: 1158–1161.
20. Nor, Z., Nor, H. and Karimah, K. **2014**. The effect of temperature on mild steel corrosion in 1 M HCl by Schiff bases, *TMJAS*, **18** (1): 28 – 36.
21. Abeng, F.E., Idim, V.D. and Nna, P.J. **2017**. Kinetics and thermodynamic studies of corrosion inhibition of mild steel using Methanolic extract of erigeron floribundus (Kunth) in 2 M HCl solution. *WVNS*, **10**: 26-38.
22. Xianglin G., Hongyuan G., Binbin Z., Weiping Z., Chao J. **2018**. Corrosion non-uniformity of steel bars and reliability of corroded RC beams. *ES*, **167**: 188–202. doi.org/10.1016/j.engstruct.2018.04.020